

On the Sunyaev-Zel'dovich effect from dark matter annihilation or decay in galaxy clusters

Julien Laval¹, Céline Boehm² and Julien Barthès²

¹*Dipartimento di Fisica Teorica, Università di Torino & INFN, via Giuria 1, 10125 Torino — Italia**

²*LAPTH, UMR 5108, 9 chemin de Bellevue - BP 110, 74941 Annecy-Le-Vieux — France†*

(Dated: today)

We revisit the prospects for detecting the Sunyaev Zel'dovich (SZ) effect induced by dark matter (DM) annihilation or decay. We show that with standard (or even extreme) assumptions for properties of the DM particles and the DM halo profile, the optical depth associated with the relativistic electrons injected from DM annihilation or decay is much smaller than that associated with the thermal electrons, when averaged over the angular resolution of current and future experiments. For example we find: $\tau_{\text{DM}} \sim 10^{-7} - 10^{-6}$ for $m_\chi = 1$ GeV and a density profile $\rho \propto r^{-1}$ for a template cluster located at 50 Mpc and observed within an angular resolution of $10''$, compared to $\tau_{\text{th}} \sim 10^{-3} - 10^{-2}$. This, together with a full spectral analysis, enables us to demonstrate that, for a template cluster with properties close to those of the nearby ones, the SZ effect due to DM annihilation or decay is far below the sensitivity of the Planck satellite. This is at variance with previous claims for heavy annihilating DM particles. Nevertheless, light DM particles with a not too suppressed annihilation or decay rate into electrons and positrons (assumed compatible with other astrophysical constraints) might still induce a deviation of the CMB spectrum observable by ALMA in the absence of other relativistic foregrounds. Finally, we provide some useful analytical formulae parameterized in terms of the DM mass, decay rate or annihilation cross section and DM halo features, that allow quick estimate of the SZ effect induced by any given candidate and any DM halo profile.

I. INTRODUCTION

The enigma of the origin of dark matter (DM) is a longstanding issue. Many experimental strategies in particle physics, astrophysics and cosmology have been developed to confirm/infirm the existing scenarios. One appealing possibility, strongly motivated by independent issues in particle physics beyond the standard model (BSM), is that DM is made of weakly interacting particles (WIMPs). The most popular models, like the supersymmetric (SUSY) neutralino (see e.g. [1, 2] for reviews), have the interesting property of self-annihilation to ordinary matter, which provides windows for the detection of the annihilation products. There is actually an impressive wealth of WIMP models, from the GeV-TeV mass-scale as in the SUSY paradigm down to the sub-GeV mass-scale, the latter class allowing, in particular, to solve the so-called *cusp* and *subhalo problems* (e.g. [3]). Since the DM annihilation or decay rate increases with the DM number density, the best targets are expected to be the centers of (sub)galaxies or galaxy clusters. This quest for annihilation or decay signals makes use of different messengers (e.g. γ -rays, antimatter cosmic rays and ν s): it is referred to as *indirect detection* of DM (for a pedagogical review, see [4]). There are of course other ways to learn about the microscopic properties of DM, for instance by detecting direct interactions of DM in ground based experiments [4], or by producing DM di-

rectly in particle colliders. All these direct and indirect detection methods have been studied at length in the literature.

Yet, a few years ago, it was pointed out in a series of papers [5, 6, 7] a new complementary method to look for DM, namely the Sunyaev-Zel'dovich (SZ) effect [8, 9]. Indeed, DM annihilation or decay in galaxy clusters may inject relativistic electrons and positrons¹ that should experience inverse Compton scattering with the CMB photons and, therefore, if numerous enough, generate a deviation to the blackbody spectrum. The question that we address in this paper is whether or not this deviation is visible in light of the contradictory results found by [5, 6, 7] on the one hand, and by [10] on the other hand. In particular, we investigate whether the Planck satellite [11], which has been recently launched, and the ALMA facilities [12, 13] will have the sensitivity to detect the SZ signal induced by DM annihilation or decay and could constrain the DM properties. Our approach provides more details than [13] on the crucial impact of the experimental angular resolution on the DM-induced SZ predictions, and also on the spectral analysis itself. We will also consider the SZ effect due to the thermal electrons lying in clusters and observed in X-ray measurements, which has been studied for a long time (see [14] for a review) and which constitutes an important background to such an exotic signature.

In this paper, we therefore revisit the calculation of the

*Electronic address: laval@to.infn.it

†Electronic address: boehm@lapp.in2p3.fr

¹ Hereafter, we will use *electron* for electron or positron, indifferently.

annihilating or decaying DM contribution to the SZ effect from nearby clusters, stressing the importance of the experimental angular resolution, and taking a template galaxy cluster located at 50 Mpc, with properties representative of all nearby clusters. Our discussion, that we will keep as generic as possible, is organized as follows. In Sec. II, we will recall the principle of the SZ calculation. In Sec. III we will derive the optical depths for both DM-induced and thermal electrons in an exact numerical manner and, likewise, provide analytical formulae to allow quick calculation of the SZ effect for any cluster and DM properties. In Sec. IV, we will then use these results together with a full spectral analysis to compute the signal due to the DM-induced electrons at the transition frequency where the thermal component is negligible, and show that the DM contribution to the SZ will be quite hardly observable with current and even future radio experiments. We will finally conclude in Sec. V.

II. PRINCIPLE

There are basically two main approaches to calculate the thermal or relativistic SZ effect, the radiative transfer method proposed in *e.g.* [15] and early formalized in [16], and the covariant Boltzmann equation formalism [17, 18, 19, 20, 21]. Recently, however, these approaches have been demonstrated to be equivalent [22, 23], which settles a self-consistent and unique framework for the SZ calculations. In the single scattering approximation, the distortion of the CMB intensity I at a photon energy E_k is given by the following equation:

$$\Delta I_\gamma(E_k) = \tau \int_0^{t_{\max}} dt (P_1(t) - \delta(t-1)) I_\gamma^0(E_k/t) \quad (1)$$

where I_γ^0 is the undistorted blackbody intensity, P_1 is the frequency redistribution function for a single electron-photon interaction and t is the ratio of scattered to unscattered photon energy. The integrand encodes the spectral features: the first term describes the spectral part that is shifted from energy E_k/t to E_k , while the second term describes the part that is removed from energy E_k to others. τ , which weights the amplitude of the distortion, is the optical depth which is related to the electron density in the cluster through the line-of-sight integral

$$\tau \equiv \sigma_T \int dl n_e(\vec{x}). \quad (2)$$

Here σ_T is the non-relativistic Thomson cross section that fully characterizes interactions of CMB photons with electrons of Lorentz factor $\gamma_e \lesssim 10^8$. As far as $\tau \ll 1$, the single scattering approximation is fully justified [23].

In order to estimate the potential of a radio experiments to detect SZ signals, however, one needs to average the optical depth within the angular resolution of the

apparatus,

$$\langle \tau \rangle_{\mu_{\text{res}}} = \frac{\sigma_T}{\Delta\Omega(\mu_{\text{res}})} \int_{\Delta\Omega(\mu_{\text{res}})} d\Omega \int dl n_e(\vec{x}), \quad (3)$$

where $\mu_{\text{res}} \equiv \cos(\theta_{\text{res}})$ characterizes the angular resolution θ_{res} .

Disregarding for the moment the spectral aspects, the observation of a relativistic SZ signal on top of the thermal contribution would roughly imply that the optical depth of the additional electron component is sizable compared to the one associated with the thermal electrons. A mere comparison of the electron densities in the cluster center, as done in [10], is indicative at 0th order. Nevertheless, because of the angular averaging, this could be misleading. Indeed, the SZ signal is in any case smeared down by angular resolution effects.

In Sec. III, we will study the effects of this averaging procedure, which is actually very common in studies on the indirect detection of DM with γ -rays (*e.g.* [24]). We will consider angular resolutions between $\sim 0.1''$ and $1'$, noticing that Planck [11] and ALMA [12, 13] could reach resolutions of $\sim 5'$ and $\sim 1''$, respectively.

Throughout the paper, moreover, we will consider the spatial distribution of the thermal electrons to be a spherical cored isothermal:

$$n_{e,\text{th}}(r) = \frac{n_{e,\text{th}}^0}{1 + \left(\frac{r}{r_c}\right)^2}, \quad (4)$$

where we will fix $n_{e,\text{th}}^0$ to 0.01 cm^{-3} , and r_c to 200 kpc. These are typical values for nearby clusters that will partly characterize our *template* cluster.

For completeness, it is worth recalling that the SZ effect is featured by the shift of the low frequency part of the CMB spectrum towards higher frequencies, but much more marginally by that of the high frequency part towards lower frequencies. This asymmetry drives ΔI to be negative at low frequencies and positive at high frequencies. The transition frequency, at which $\Delta I = 0$, is intimately related to the energy spectrum of the involved electron gas. Because the thermal and DM-induced components are found in different energy ranges, the associated transition frequencies are different. Therefore, not only do we need to compare the optical depths of both contributions, that weight the amplitudes of the corresponding distortions, but also to study the spectral features of ΔI . For the spectral study, we will mainly focus on ΔI_χ at the transition frequency of the thermal component ($\Delta I_{\text{th}} = 0$) in Sec. IV.

III. INJECTED ELECTRON DENSITY FROM DM ANNIHILATION OR DECAY AND OPTICAL DEPTHS

The injection rate of relativistic electrons (and positrons) from DM annihilation or decay characterizes

distance (Mpc)	R_{vir} (kpc)	r_s and r_c (kpc)	ρ_s (GeV/cm ³)	thermal e^- density (cm ⁻³)
50	1000	200	0.01	0.01

Table I: Properties of the *template* cluster used in this paper.

a nominal source term

$$\mathcal{Q}_{n,\gamma}(E, \vec{x}) = N_0 \alpha_n \left(\frac{\rho_\gamma(\vec{x})}{m_\chi} \right)^n \mathcal{F}(E), \quad (5)$$

where N_0 is the total number of electrons and positrons injected per annihilation or decay in the relevant energy range, $\mathcal{F}(E)$ is the energy spectrum normalized to unity, and m_χ is the DM particle mass. The index n is 1 or 2 for DM decay or annihilation, respectively. Therefore, $\alpha_1 \equiv \Gamma_\chi$ is a decay rate, while $\alpha_2 \equiv \delta \langle \sigma v \rangle / 2$ ($\delta = 1$ or $1/2$ for Majorana or Dirac fermions, 1 for bosons) is an annihilation rate. The DM mass density profile ρ_γ is indexed by its inner logarithmic slope γ , and is usually written like a spherical symmetric component with a scale radius r_s and a scale density ρ_s [25]

$$\rho_\gamma(r) = \frac{\rho_s (r_s/r)^\gamma}{(1 + (r/r_s)^\alpha)^{(\beta-\gamma)/\alpha}} = \rho_s f_\gamma(r). \quad (6)$$

The so-called Navarro-Frenk-White (NFW) profile [26] corresponds to $(\alpha, \beta, \gamma) = (1, 3, 1)$, while the Moore profile [27] is even more cuspy with $(1.5, 3, 1.5)$. Notice that a cored isothermal profile with $(2, 2, 0)$ is equivalent to the thermal electron distribution of Eq. (4), with $r_s = r_c$; this might be kept in mind with further benefit. We will study all of the three aforementioned profiles in the following, for both annihilating and decaying DM models. The typical values of the scale parameters found for galaxy clusters in cosmological N-body simulations are $r_s \sim 200$ kpc and $\rho_s \sim 0.01 \text{ GeV.cm}^{-3}$ (*e.g.* [28]). We will adopt these parameters for the *template* cluster that we will use for our calculations throughout this paper. We summarize them in Tab. I.

After their injection in the intracluster medium, relativistic electrons and positrons diffuse in space and momentum. The main processes that come into play are the energy losses, with a typical timescale ~ 300 Myrs, and the spatial diffusion due to scatters with the magnetic inhomogeneities. It was shown in previous analyses that since the relevant spatial diffusion scale is \sim kpc, which is just a bit larger than typical resolution scales, one can neglect spatial diffusion at first order [7]. We will stick to this approximation, for which, in steady state, the diffusion equation reduces to

$$\frac{\partial}{\partial E} \left\{ b(E) \frac{dn_{e,\chi}^{n,\gamma}(E, \vec{x})}{dE} \right\} = \mathcal{Q}_{n,\gamma}(E, \vec{x}), \quad (7)$$

where $b(E) \equiv -dE/dt$ is the energy loss rate. This equa-

tion is easily solved:

$$\begin{aligned} \frac{dn_{e,\chi}^{n,\gamma}(E, \vec{x})}{dE} &= \frac{1}{b(E)} \int_E^{m_\chi} dE_s \mathcal{Q}_{n,\gamma}(E_s, \vec{x}) \\ &= \frac{N_0 \alpha_n}{b(E)} \left(\frac{\rho_\gamma(\vec{x})}{m_\chi} \right)^n \int_E^{m_\chi} dE_s \mathcal{F}(E_s). \end{aligned} \quad (8)$$

Now, to compute the optical depth, as defined in Eq. (2), we need to integrate this differential electron density over energy. From the previous equation, this gives:

$$n_{e,\chi}^{n,\gamma}(\vec{x}) = N_0 \alpha_n \left(\frac{\rho_\gamma(\vec{x})}{m_\chi} \right)^n \int_{E_{\text{min}}}^{m_\chi} \frac{dE}{b(E)} \int_E^{m_\chi} dE_s \mathcal{F}(E_s). \quad (9)$$

We can further express the energy loss rate as $b(E) = (E_0/\tau_{\text{loss}})/g(E)$, where $E_0 = 1$ GeV, τ_{loss} is the typical energy loss timescale, and $g(E)$ is a dimensionless function that encodes the energy dependence of the energy loss rate. The previous equation is then more conveniently rewritten as

$$n_{e,\chi}^{n,\gamma}(\vec{x}) = N_0 \alpha_n \left(\frac{\rho_\gamma(\vec{x})}{m_\chi} \right)^n \tau_{\text{loss}} \bar{\mathcal{F}}, \quad (10)$$

where we have defined

$$\bar{\mathcal{F}} \equiv \int_{E_{\text{min}}}^{m_\chi} \frac{dE}{E_0} g(E) \int_E^{m_\chi} dE_s \mathcal{F}(E_s). \quad (11)$$

Note that $\bar{\mathcal{F}} \approx m_\chi/E_0$ for Coulomb losses ($g(E) \propto cst$), while $\bar{\mathcal{F}} \approx E_0/E_{\text{min}}$ for inverse Compton losses ($g(E) \propto (E/E_0)^2$), which is in any case $\lesssim 10^3$.

Now, to go further in our calculation of the optical depth, we need to compute the average density of electrons within the angular resolution of the telescope.

A. Line-of-sight averaged optical depth and electron density

As stated in Sec. II through Eq. (3), the optical depth must be averaged within the experimental angular resolution. The full line-of-sight integral is not analytical in most of cases. We can reexpress Eq. (3) in such a way that an averaged electron density explicitly appears:

$$\langle \tau_{e,\chi}^{n,\gamma} \rangle = 2 r_s \sigma_T \widetilde{\langle n_{e,\chi}^{n,\gamma} \rangle}_{\text{res}}. \quad (12)$$

The scale radius r_s just translates the fact that the most important contribution to the SZ is expected to come within a distance of r_s upwards and downwards from the cluster center along the line-of-sight (explaining thus the factor of 2). This is essentially true for annihilating dark matter, but the equation is anyway made exact for all cases by defining the average electron density as

$$\widetilde{\langle n_{e,\chi}^{n,\gamma} \rangle}_{\text{res}} = N_0 \alpha_n \left(\frac{\rho_s}{m_\chi} \right)^n \tau_{\text{loss}} \bar{\mathcal{F}} \mathcal{J}^{n,\gamma}. \quad (13)$$

This ensures Eq. (12) to be an exact formulation of the angular averaging of the optical depth, provided a proper definition of the dimensionless parameter $\mathcal{J}^{n,\gamma}$, which carries the angular average:

$$\begin{aligned} \mathcal{J}^{n,\gamma} &\equiv \frac{1}{2r_s(1-\mu_{\text{res}})} \int_{\mu_{\text{res}}}^1 d\mu \int dl (f_\gamma(r(l,\mu)))^n \\ &= \frac{1}{2r_s(1-\mu_{\text{res}})} \int_{\mu_{\text{res}}}^1 d\mu \times \\ &\quad 2 \int_0^{\sqrt{R_{\text{vir}}^2 - b^2}} ds (f_\gamma(r(s,b)))^n \\ &= \frac{(1+\mu_{\text{res}})}{b_{\text{res}}^2} \int_0^{b_{\text{res}}} \frac{db b}{\sqrt{1 - \frac{b^2}{D^2}}} \times \\ &\quad \int_0^{\sqrt{R_{\text{vir}}^2 - b^2}} \frac{ds}{r_s} \left(f_\gamma(\sqrt{s^2 + b^2}) \right)^n. \end{aligned} \quad (14)$$

$b = D \sin(\theta_{\text{res}})$ is the impact parameter, $\mu_{\text{res}} = \cos(\theta_{\text{res}})$, $f_\gamma(r) \equiv \rho_\gamma(r)/\rho_s$, $s \equiv \sqrt{r^2 - b^2}$ is the reduced line-of-sight variable and R_{vir} is the virial radius of the cluster. We have expressed the angular integral in terms of an integral over the impact parameter, which allows a better control of numerical aspects. It is usually convenient to integrate over b and s with logarithmic steps, and to define a numerical cut r_{cut} for f_γ when $b \rightarrow 0$. Though formally set, in a pure DM halo, by equating the gravitational infall timescale with the annihilation timescale [29], r_{cut} can be chosen to ensure a good compromise between numerical accuracy, convergence and computing time, but in any case should obey $r_{\text{cut}} \ll b_{\text{res}}$. We remind, nevertheless, that small core radii could instead arise from other non-trivial dynamical effects involving baryons, and are actually observed at the galactic scale [30].

With the previous definitions, simple estimates of the optical depths associated with DM decay and annihilation read, respectively:

$$\begin{aligned} \langle \tau_{e,\chi}^{1,\gamma} \rangle_{\text{res}}^{\text{dec}} &= \tau_{0,\chi}^{\text{dec}} \frac{N_0}{10} \frac{\bar{\mathcal{F}}}{10^3} \frac{\Gamma_\chi}{10^{-26} \text{s}^{-1}} \frac{\tau_{\text{loss}}}{10^{17} \text{s}} \times \\ &\quad \left(\frac{\rho_s / (0.01 \text{ GeV/cm}^3)}{m_\chi / \text{GeV}} \right) \left(\frac{2r_s \mathcal{J}^{1,\gamma}}{10^3 \text{ kpc}} \right) \\ \langle \tau_{e,\chi}^{2,\gamma} \rangle_{\text{res}}^{\text{ann}} &= \tau_{0,\chi}^{\text{ann}} \frac{N_0}{10} \frac{\bar{\mathcal{F}}}{10^3} \frac{\langle \sigma v \rangle}{3 \cdot 10^{-26} \text{ cm}^3 \text{ s}^{-1}} \frac{\tau_{\text{loss}}}{10^{17} \text{ s}} \times \\ &\quad \left(\frac{\rho_s / (0.01 \text{ GeV/cm}^3)}{m_\chi / \text{GeV}} \right)^2 \left(\frac{2r_s \mathcal{J}^{2,\gamma}}{10^5 \text{ kpc}} \right), \end{aligned} \quad (15)$$

where the typical optical depths are given by

$$\begin{aligned} \tau_{0,\chi}^{\text{dec}} &= 2.05 \cdot 10^{-7} \\ \tau_{0,\chi}^{\text{ann}} &= 3.07 \cdot 10^{-7}. \end{aligned} \quad (16)$$

It is important to note that the values that we have taken for N_0 and $\bar{\mathcal{F}}$ typify mostly DM particles with masses

above ~ 100 MeV, since for lighter particles, the annihilation or decay will be mostly into light fermion pairs. For direct annihilation or decay in e^+e^- , we would have $N_0 = 2$ and $\bar{\mathcal{F}} \approx 1$ (see Sec. IV), which would reduce the previous estimates of the optical depths by a factor of $5 \times 10^3!$

In Fig. 1, we plot the full results. We have sketched the behaviors of the exact computation of $\tilde{\mathcal{J}}^{n,\gamma} \equiv 2r_s \mathcal{J}^{n,\gamma}$ on the one hand, and of the corresponding analytical spherical / line-of-sight approximations derived in Sec. III B on the other hand, as functions of the resolution angle (or the corresponding impact parameter, which allows to deal with physical distances — see the top horizontal axis). These results are translated in terms of optical depth by means of the DM properties used in Eq. (15). Note that larger values of R_{vir} would not affect the results, since the denser part of the DM distribution is within r_s . Different values of the cluster distance D would affect the scaling of horizontal axis, the closer cluster the better the spatial resolution.

The values of the DM-induced electron optical depths derived in Eq. (15) have to be compared with what is expected for the thermal electrons. Because the latter obey an isothermal cored profile, as made explicit in Eq. (4), the function $\mathcal{J}^{1,0}$ can be used to infer their optical depth (we take advantage of that we have used $r_c = r_s$). We find:

$$\langle \tau \rangle_{\text{res}}^{\text{th}} = \tau_{0,\text{th}} \left(\frac{n_{e,\text{th}}^0}{0.01 \text{ cm}^{-3}} \right) \left(\frac{2r_c \mathcal{J}^{1,0}}{10^3 \text{ kpc}} \right), \quad (17)$$

where the typical optical depth is found to be

$$\tau_{0,\text{th}} = 2.05 \cdot 10^{-2} \quad (18)$$

with our template parameters. Such a value is very close to what is actually found in dedicated studies, where $\tau \sim 10^{-3} - 10^{-2}$ [14]. Moreover, this value remains a constant function of angular the resolution up to an angular size that corresponds, roughly, to the core radius $r_c \sim 200$ kpc.

If at first glance, still disregarding the spectral aspects, we want to compare the thermal and DM optical depths, then we can use Fig. 1 (the left vertical axis gives $2r_s \mathcal{J}^{n,\gamma}$ and the right vertical axis provides the translation in terms of optical depth for annihilating DM with the generic parameters used in Eq. 15). From this figure, we can already emphasize that unless $\langle \sigma v \rangle \gg 3 \cdot 10^{-26} \text{ cm}^3/\text{s}$, $\Gamma_\chi \gg 10^{-26} \text{ s}^{-1}$ or $m_\chi \ll 1$ GeV, $\gamma > 1$ or $\rho_s \gg 0.01 \text{ GeV/cm}^3$, DM decay or annihilation cannot supply a sufficient amount of electrons to compete with the thermal optical depth, even with rather light DM particles in the sub-GeV mass-scale with other conventional parameters. This statement is in qualitative agreement with [10], though based on more accurate averaging calculations, but in clear disagreement with [5, 6, 7]. The potential of future experiments for detection, with an angular resolution $\sim 1''$, seems to arise only for light DM with $m_\chi < 1$ GeV, either with

rather large annihilation or decay rates, or distributed with very cuspy profiles à la Moore ($\gamma = 1.5$), which is now strongly disfavored from the most recent cosmological N-body simulations (e.g. [31]).

Before tackling the full spectral analysis, we derive hereafter some approximated analytical expressions of the line-of-sight integral $\mathcal{J}^{n,\gamma}$. This set of *fast* formulae is aimed at providing some quick estimates of the optical depth for any annihilating or decaying DM model, and for any density profile discussed below Eq. (6).

B. Analytical approximations

The relevant part of the DM distribution is that within the angular resolution of the telescope. The current and foreseen angular resolutions are not better than $\theta_{\text{res}} \sim 1''$. Because clusters lie at distances around 50 Mpc, the spatial resolution is therefore not smaller than $b_{\text{res}} \sim D \theta_{\text{res}} \sim 0.1$ kpc (b is defined as the impact parameter). Such values are much smaller than the typical scale radii r_s found for cluster density profiles, so we can approximate the density profile of Eq. (6) as

$$\begin{aligned} \rho_\gamma(r) &\approx \rho_s \left(\frac{r_s}{r}\right)^\gamma \\ \Leftrightarrow f_\gamma(r) &\approx \left(\frac{r_s}{r}\right)^\gamma. \end{aligned} \quad (19)$$

Beside the fact that the impact parameter is, in most cases, smaller than the scale radius r_s , this approximation is further justified from that the dominant part of the line-of-sight dark matter contribution arises within a sphere of radius r_s by the cluster center (the argument is weaker for decaying DM). We will therefore disregard the whole spatial extent of the cluster characterized by R_{vir} , and focus only on the region within r_s . We further assume $D \gg r_s \gg b_{\text{res}} \gg r_{\text{cut}}$. This latter cut-off radius r_{cut} has already been discussed below Eq. (14). It has no impact except for diverging injection rates, scaling like $r^{-\alpha}$ with $\alpha \geq 3$ (corresponding for instance to annihilating DM distributed with a Moore profile); we will use $r_{\text{cut}} = 10^{-3}$ pc in the following. We will develop two types of approximations, one based on a spherical average, the other based on a more accurate line-of-sight treatment.

1. The spherical approximation

If the impact parameter is sufficiently small, the average value of the electron density determined in Eq. (13) can be approximated by a spherical integral of $n_{e,\chi}$ around b_{res} , weighted by the conic volume $\sim \pi b_{\text{res}}^2 R_{\text{vir}}/3$ of the cluster roughly carried by the telescope resolution. In this case, we can derive a spherical approximation of

the dimensionless function $\mathcal{J}^{n,\gamma}$ as follows

$$\begin{aligned} \mathcal{J}^{n,\gamma} &\approx \mathcal{J}_{\text{sph}}^{n,\gamma} \\ &\approx \frac{12}{b_{\text{res}}^2 R_{\text{vir}}} \frac{R_{n,\beta,\gamma}}{r_s} r_s^{n\gamma} \begin{cases} \frac{r_s^{3-n\gamma}}{3-n\gamma} \Big|_{r_{\text{cut}}}^{b_{\text{res}}}, & n\gamma \neq 3 \\ \ln\left(\frac{b_{\text{res}}}{r_{\text{cut}}}\right) & \text{otherwise} \end{cases} \end{aligned} \quad (20)$$

A given product of $n\gamma$ corresponds to one or two DM configurations, as recalled in Tab. II. The scaling with b_{res} is found to match exactly the actual behavior of $\mathcal{J}^{n,\gamma}$, but we need to define and tune a new scale, $R_{n,\beta,\gamma}$, to get closer to the actual value of the optical depth ($\beta = 3$ for the NFW and Moore profiles, and $\beta = 2$ for cored isothermal profiles). $R_{n,\beta,\gamma}$ should be of the order r_s for consistency reasons (see Eqs. 12 and 13). We actually find that

$$R_{n,\beta,\gamma} = r_{n,\gamma}^0 \left(\frac{b_{\text{res}}}{r_{n,\gamma}}\right)^{\beta-3} \quad (21)$$

with

$$\begin{aligned} r_{1,\gamma}^0 &= r_s \quad r_{1,\gamma} = \frac{r_s}{7} \\ r_{2,\gamma}^0 &= r_{2,\gamma} = r_s, \end{aligned} \quad (22)$$

provides a reasonable approximation of the accurate numerical results, by less than one order of magnitude for cluster parameters not too far from those of our template model. This is therefore consistent with the values expected for $R_{n,\beta,\gamma}$. The comparison with the accurate result is shown in Fig. 1. Although this approximation allows to derive orders of magnitude quite quickly, we recall that it is very simplistic, so one should use it with care. We recommend not to use it for very detailed analyses, but instead to make the full computation of Eq. (12). The line-of-sight approximation derived in the next paragraph will turn out to be more accurate, but the spherical case is more intuitive.

2. The line-of-sight approximation

With the same approximation as above (see Eq. 19), one can also try to find analytical solutions of the line-of-sight integral of Eq. (14). Assuming that the impact parameter $b \ll r_s \ll D$, which is always the case for typical angular resolutions, we can write $\mathcal{J}^{n,\gamma} \approx \mathcal{J}_{\text{los}}^{n,\gamma}$, where:

$$\mathcal{J}_{\text{los}}^{n,\gamma} \equiv \frac{(1 - \mu_{\text{res}})}{b_{\text{res}}^2} \int_0^{b_{\text{res}}} db b \int_0^{r_s} \frac{ds}{r_s} \left(\frac{r_s^2}{s^2 + b^2}\right)^{n\gamma/2}. \quad (23)$$

The upper bound of the integral over s is r_s and not R_{vir} to be consistent with the validity domain of our current approximations. The different possible combinations of $n\gamma$ are recalled in Tab. II.

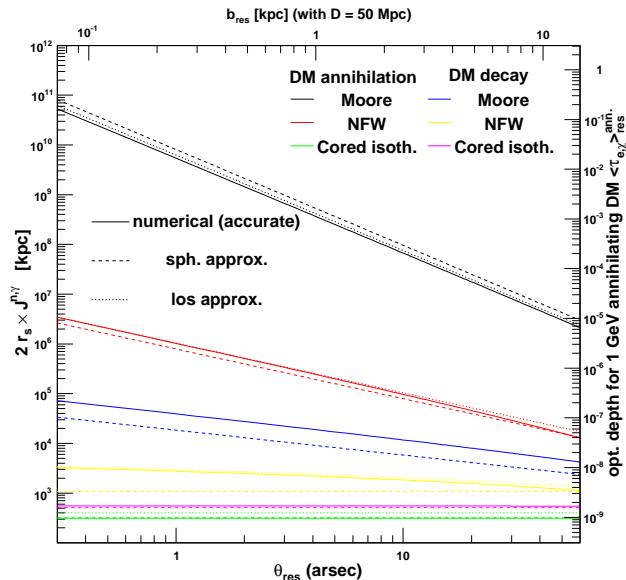


Figure 1: Line-of-sight integral for the accurate numerical computation, the spherical approximation and the so-called line-of-sight approximation, as a function of the angular resolution over which it is averaged. The bottom horizontal axis is the angular resolution, the top vertical one is the corresponding impact parameter $b_{\text{res}} = D \sin(\theta_{\text{res}})$. The left vertical axis is $2r_s \mathcal{J}^{n,\gamma}$ — see Sec. III A — while the right vertical axis translates those values in terms of optical depth for typical DM parameters, but only for annihilating DM (the optical depth axis for decaying DM would be a factor of ~ 1.5 smaller, for nominal parameters — see Eq. 15).

nature / profile	cored ($\gamma = 0$)	NFW ($\gamma = 1$)	Moore ($\gamma = 3/2$)
decaying ($n = 1$)	0	1	3/2
annihilating ($n = 2$)	0	2	3

Table II: Various combinations of the product $n\gamma$ and associated DM configurations for the analytical functions $\mathcal{J}_{\text{sph.}}^{n\gamma}$ and $\mathcal{J}_{\text{los}}^{n\gamma}$ (see Secs. III B 1 and III B 2).

Using Eqs. (15) and (17), the ratio of the DM to thermal optical depths is proportional to $\mathcal{J}_{\text{los}}^{1(2)}/\mathcal{J}_{\text{los}}^0$, for decaying (annihilating) DM. More explicitly, we get, for decaying DM,

$$\begin{aligned} \eta_{\chi}^{\text{dec}} &\equiv \frac{\langle \tau_{e,\chi} \rangle_{\text{res}}^{\text{dec}}}{\langle \tau_{e,\text{th}} \rangle_{\text{res}}} = \frac{\tau_{0,\chi}^{\text{dec}}}{\tau_{0,\text{th}}} \left(\frac{n_{e,\text{th}}^0}{0.01 \text{ cm}^{-3}} \right)^{-1} \frac{N_0}{10} \frac{\bar{\mathcal{F}}}{10^3} \frac{\Gamma_{\chi}}{10^{-26} \text{ s}^{-1}} \frac{\tau_{\text{loss}}}{10^{17} \text{ s}} \left(\frac{\rho_s / (0.01 \text{ GeV/cm}^3)}{m_{\chi} / \text{GeV}} \right) \left(\frac{\mathcal{J}_{\text{los}}^1}{\mathcal{J}_{\text{los}}^0} \right) \\ &= \eta_{\chi}^{0,\text{dec}} \left(\frac{n_{e,\text{th}}^0}{0.01 \text{ cm}^{-3}} \right)^{-1} \frac{N_0}{10} \frac{\bar{\mathcal{F}}}{10^3} \frac{\Gamma_{\chi}}{10^{-26} \text{ s}^{-1}} \frac{\tau_{\text{loss}}}{10^{17} \text{ s}} \left(\frac{\rho_s / (0.01 \text{ GeV/cm}^3)}{m_{\chi} / \text{GeV}} \right) \ln \left(\frac{2(r_s/200 \text{ kpc})}{b_{\text{res}}/1 \text{ kpc}} \right), \end{aligned} \quad (25)$$

with

$$\eta_{\chi}^{0,\text{dec}} = 5.99 \cdot 10^{-5}. \quad (26)$$

The function $\mathcal{J}_{\text{los}}^{n\gamma}$ can be computed analytically in the following cases:

$$\begin{aligned} \mathcal{J}_{\text{los}}^0 &= \frac{(1 + \mu_{\text{res}})}{2} \\ \mathcal{J}_{\text{los}}^1 &= \frac{(1 + \mu_{\text{res}})}{2} \ln \left(\frac{2r_s}{b_{\text{res}}} \right) \\ \mathcal{J}_{\text{los}}^2 &= \frac{(1 + \mu_{\text{res}})\pi}{2} \frac{r_s}{b_{\text{res}}} \\ \mathcal{J}_{\text{los}}^3 &= (1 + \mu_{\text{res}}) \left(\frac{r_s}{b_{\text{res}}} \right)^2 \ln \left(\frac{b_{\text{res}}}{(1 + \sqrt{2})r_{\text{cut}}} \right). \end{aligned} \quad (24)$$

Armed with these equations, the approximated optical depths are merely proportional to $2r_s \mathcal{J}_{\text{los}}^{n\gamma}$, as given in Eqs. (12) and (13). The results are also reported in Fig. 1, where the agreement with the exact calculation is shown to be quite good.

C. Thermal to DM optical depth ratio η_{χ}

To size the relative amplitude of the SZ distortion induced by DM annihilation or decay on top of the thermal component, it is useful to derive the ratio $\eta_{\chi} \equiv \langle \tau_{e,\chi} \rangle_{\text{res}} / \langle \tau_{e,\text{th}} \rangle_{\text{res}} \gtrsim 0.1$, at any frequency where $\Delta I_{\text{th}} \neq 0$. Since the frequency where ΔI crosses 0 is different for each electron component, it is further important to compare the absolute amplitude of ΔI_{χ} , at the frequency where $\Delta I_{\text{th}} = 0$, with the current experimental sensitivities, *i.e.* $\Delta I/I \sim 10^{-6}$. We will estimate the ratio η_{χ} below, but postpone our discussion of the latter point in Sec. IV. For the sake of clarity, we will base the following calculation on the assumption that the DM density profile is an NFW ($\gamma = 1$). Likewise, we will use the analytical line-of-sight approximation derived in the previous section, which turns out to be the most precise.

For annihilating DM, the result is proportional to $\mathcal{J}_{\text{los}}^2/\mathcal{J}_{\text{los}}^0$, and we have instead

$$\begin{aligned} \eta_\chi^{\text{ann}} &\equiv \frac{\langle \tau_{e,\chi}^{1,1} \rangle_{\text{res}}^{\text{ann}}}{\langle \tau_{e,\text{th}} \rangle_{\text{res}}} \\ &= \eta_\chi^{0,\text{ann}} \left(\frac{n_{e,\text{th}}^0}{0.01 \text{ cm}^{-3}} \right)^{-1} \frac{N_0}{10} \frac{\bar{\mathcal{F}}}{10^3} \frac{\langle \sigma v \rangle}{3 \cdot 10^{-26} \text{ cm}^3 \text{ s}^{-1}} \frac{\tau_{\text{loss}}}{10^{17} \text{ s}} \left(\frac{\rho_s / (0.01 \text{ GeV/cm}^3)}{m_\chi / \text{GeV}} \right)^2 \left(\frac{r_s / 200 \text{ kpc}}{b_{\text{res}} / 1 \text{ kpc}} \right), \end{aligned} \quad (27)$$

where

$$\eta_\chi^{0,\text{ann}} = 9.41 \cdot 10^{-5}. \quad (28)$$

The relevant parameters here are $\eta_\chi^{0,\text{dec}}$ and $\eta_\chi^{0,\text{ann}}$, which both are $\ll 0.1$ for most of DM models and for current and future experimental performances. Because the optical depth weights the amplitude of the spectral distortion (see Eq. 1), this means that detecting a SZ signal from DM annihilation or decay on top of the thermal contribution demands very strong spectral distortions of the former with respect to the latter. We study the spectral features of the SZ signatures in the next section.

IV. SPECTRAL DISTORTION ANALYSIS

To complete our study, we have to tackle a full spectral analysis. Nevertheless, what is quantitatively interesting is the amplitude of the spectral change due to DM at the SZ transition frequency of the thermal gas, *i.e.* when its global effect is null. In this section, therefore, we estimate the amplitude of ΔI_χ at the frequency at which $\Delta I_{\text{th}} = 0$, to size the potential impact of DM at the transition frequency of the thermal background. We adopt the formalism developed in [32], which is very well suited for our calculation. We refer the reader to that article for more details on the quantities and results that are used below.

Let us first define the reduced blackbody intensity $i(x) \equiv I(E_k)/i_0 = x^3/(e^x - 1)$, where $x \equiv E_k/(kT_0)$, T_0 is the CMB temperature, and $i_0 \equiv 2(kT_0)^3/(hc)^2$. With these notations, Eq. (1) can be rewritten in terms of the reduced intensities

$$\delta i(x) = \tau (j(x) - i(x)), \quad (29)$$

where we further define the scattered photon intensity as:

$$j(x) \equiv \int_0^{t_{\text{max}}} dt P_1(t) i(x/t). \quad (30)$$

The photon frequency redistribution function $P_1(t)$, valid in the single scattering approximation, depends on the normalized injected electron spectrum $\mathcal{F}(E) = \mathcal{F}(\bar{p})$ ($\bar{p} \equiv p/(m_e c) = \gamma_e \beta_e = \sqrt{\gamma_e^2 - 1}$ being the reduced electron momentum) as follows:

$$P_1(t) = \int d\bar{p} \mathcal{F}(\bar{p}) P_1(t, \bar{p}), \quad (31)$$

where $P_1(t, \bar{p})$ has the following analytical form

$$\begin{aligned} P_1(t, \bar{p}) &= -\frac{3|1-t|}{32\bar{p}^6 t} \left\{ 1 + (10 + 8\bar{p}^2 + 4\bar{p}^4)t + t^2 \right\} + \quad (32) \\ &\frac{3(1+t)}{8\bar{p}^5} \left\{ \frac{3 + 3\bar{p}^2 + \bar{p}^4}{\sqrt{1 + \bar{p}^2}} - \frac{3 + 2\bar{p}^2}{\bar{p}} \left(\text{asinh}(\bar{p}) - \frac{|\ln(t)|}{2} \right) \right\}. \end{aligned}$$

The maximal frequency shift, above which $P_1(t, \bar{p}) = 0$, fulfills the condition $|\ln(t_{\text{max}})| = 2 \text{asinh}(\bar{p})$.

Armed with these equations, we can derive the intensity shift δi for any electron component, given its spectrum. For the thermal electrons, we will use a Maxwell-Boltzmann spectrum

$$\mathcal{F}_{\text{th}}(\bar{p}) = \frac{\beta_{\text{th}}}{K_2(\beta_{\text{th}})} \bar{p}^2 \exp\left(-\beta_{\text{th}} \sqrt{1 + \bar{p}^2}\right), \quad (33)$$

where $\beta_{\text{th}} = m_e c^2/(kT_{\text{th}})$ is the inverse reduced electron temperature, and where the normalization is ensured with the modified Bessel function of the second kind K_2 . The resulting redistribution function (see Eq. 31) is shown in Fig. 2, for different temperatures.

For the DM electron yield, we will assume that the injected spectrum is $\propto \delta(E - n m_\chi/2)$, with $n = 1$ or 2 for decay or annihilation, respectively. This is equivalent to assuming a direct annihilation or decay in e^+e^- , which is particularly relevant for light DM particles and thereby a conservative hypothesis. We can thus determine the normalized equilibrium spectrum with Eq. (9):

$$\mathcal{F}(E) = \frac{K}{b(E)} \quad (\text{for } E \leq m_\chi), \quad (34)$$

where $K = K(E_{\text{min}}, E_{\text{max}})$ is a normalization constant such that $\int dE \mathcal{F}(E) = 1$ in the energy range of interest. For the energy loss rate $b(E)$, we can combine the two most relevant regimes, *i.e.* the Coulomb losses below $E_0 = 1 \text{ GeV}$, of timescale τ_{Coul} and the inverse Compton losses on CMB above [33], of timescale τ_{IC} . Actually, we

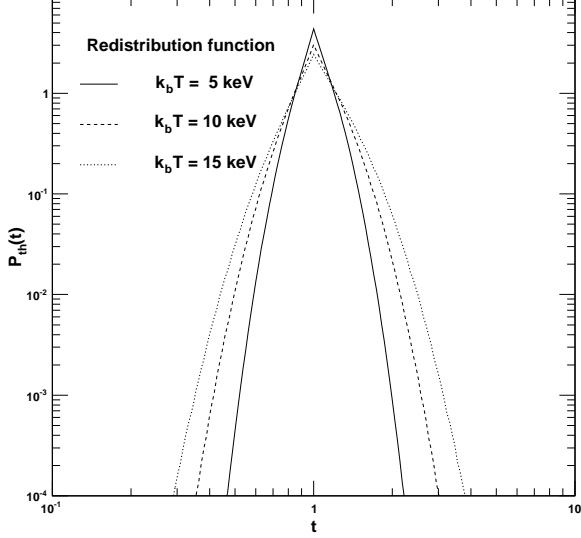


Figure 2: Frequency redistribution function for different thermal electron gas temperatures, $kT_{\text{th}} = 5, 10, 15$ keV.

have:

$$\begin{aligned} \frac{b(E)}{10^{-16} \text{GeV/s}} &= b_{\text{IC}}(E) + b_{\text{Coul.}}(E) \\ &= 0.265 \left(\frac{E}{E_0} \right)^2 + \\ &\quad \frac{6.20}{\beta_e} \frac{n_{e,\text{th}}}{1 \text{ cm}^{-3}} \left\{ 1 + \ln \left(\frac{E/E_0}{n_{e,\text{th}}/1 \text{ cm}^{-3}} \right) \right\}, \end{aligned} \quad (35)$$

where the Coulomb loss rate is taken from [34]. We can simplify the previous expression by means of the timescales

$$\begin{aligned} b(E) &\simeq \frac{E_0}{\tau_{\text{Coul.}}} + \frac{E^2}{E_0 \tau_{\text{IC}}} = \frac{E_0}{\tau_{\text{Coul.}}} \left\{ \alpha_\tau \left(\frac{E}{E_0} \right)^2 + 1 \right\} \\ \frac{\tau_{\text{Coul.}}}{10^{16} \text{ s}} &\equiv 0.16 \times \frac{\beta_e}{n_{e,\text{th}}/1 \text{ cm}^{-3}}, \quad \frac{\tau_{\text{IC}}}{10^{16} \text{ s}} \equiv 3.77 \\ \alpha_\tau &\equiv \frac{\tau_{\text{Coul.}}}{\tau_{\text{IC}}}. \end{aligned} \quad (36)$$

With this form of energy loss rate, we can reexpress Eq. (34) as

$$\mathcal{F}(E) = \frac{K(E_{\text{min}}, m_\chi) \tau_{\text{coul}}}{\alpha_\tau \frac{E^2}{E_0^2} + 1}. \quad (37)$$

The correspondence between energy and reduced momentum is straightforward: $\bar{p} = \sqrt{\gamma_e^2 - 1}$, and $dE = \bar{p} m_e^2 c^4 d\bar{p}/E$. The energy lower bound E_{min} must be consistent with the cluster age, DM-induced electrons

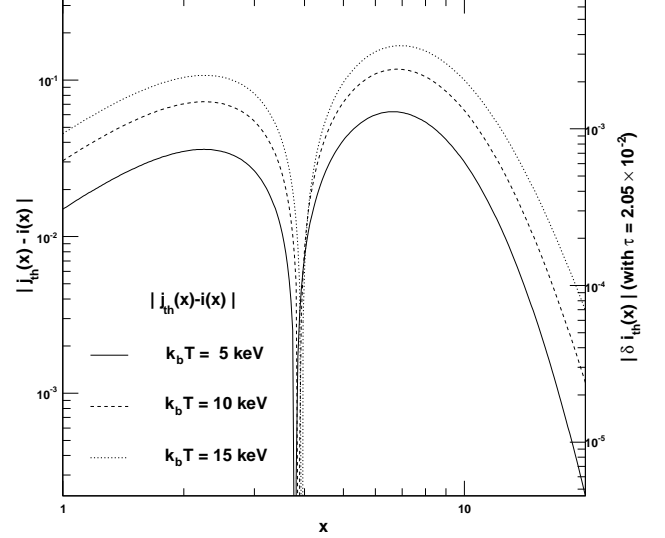


Figure 3: $\delta i_{\text{th}}(x)/\tau$ for different thermal electron gas temperatures, $kT_{\text{th}} = 5, 10, 15$ keV (the right vertical axis gives $|\delta i_{\text{th}}(x)|$ for our template cluster, with an optical depth of $\tau = 2.05 \times 10^{-2}$).

having essentially been injected since the cluster has formed. Therefore, those electrons had only a time of the order of the cluster age $\Delta t \approx t_{\text{cl}} - t_{\text{em.}} \approx t_{\text{cl}}$ to lose their energy. We can compute the minimal energy $E_{\text{min}} \geq m_e c^2$ corresponding to any injected energy E by demanding $\int_{E_{\text{min}}}^E dE' \frac{E_0}{b(E')} \leq \Delta t$, which is equivalent to $K^{-1}(E_{\text{min}}, E) \leq \Delta t$. For typical cluster formation redshifts around 5, E_{min} is merely found to be $m_e c^2$.

The photon redistribution function obtained from the DM-induced electrons, once the normalized spectrum defined in Eq. (34) has been injected into Eq. (31), is shown in Fig. 4, for different WIMP masses, assuming direct annihilation or decay in e^+e^- .

Notice that when coming to the numerical calculation of the optical depth, we will take advantage of the estimates performed in the previous section by remarking that the function $\bar{\mathcal{F}}$ defined in Eq. (11) obeys rigorously $\tau_{\text{loss}} \bar{\mathcal{F}} = K^{-1}(E_{\text{min}}, m_\chi)$, in the current DM configuration. If we assume that $\tau_{\text{loss}} \approx \tau_{\text{coul}} \approx \tau_{\text{ic}}$, then we have $\bar{\mathcal{F}} \approx 1$. Hence, with such an assumption, we can rescale the optical depths given in Eq. (16) accordingly.

Our aim is to size $\delta i_\chi(x_{\text{th}})$ at a frequency x_{th} such that $\delta i_{\text{th}}(x_{\text{th}}) = 0$. x_{th} is readily found by computing Eq. (29), given the thermal electron temperature. For completeness, we take three different temperatures, $kT_{\text{th}} = 5, 10, 15$ keV, though it is well known that the transition frequency is much less dependent on the temperature than the amplitude, as shown in Fig. 3. As illustrated in that plot for the three cases, we find $x_{\text{th}} \simeq 4$.

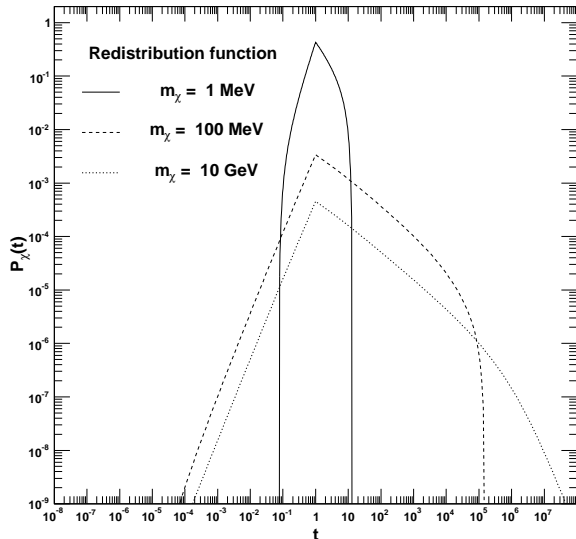


Figure 4: Redistribution functions for different WIMP masses, assuming $\chi\chi \rightarrow e^+e^-$. Decaying DM functions are identical for $\chi \rightarrow e^+e^-$ but with twice the indicated masses.

We can now calculate

$$\delta i_\chi(x_{\text{th}}) = \tau_\chi (j_\chi(x_{\text{th}}) - i(x_{\text{th}})), \quad (38)$$

with

$$j_\chi(x_{\text{th}}) = \int_0^{t_{\text{max}}} dt P_1(t, \bar{p}_\chi) i(x/t), \quad (39)$$

and for different DM particle masses.

We first report the behavior obtained for $\delta i_\chi(x)/\tau_\chi$ with different WIMP masses in Fig. 5, assuming direct annihilation in e^+e^- (also valid for decaying DM, but with twice the masses). The factor of $1/\tau_\chi$ allows a prediction independent of the electron density, *i.e.* independent of the cluster halo parameters. The right vertical axis gives the conversion in terms of $\delta i_\chi(x)$, assuming $\tau_\chi = 6.1 \times 10^{-11}$ (see below), which reaches a maximum of $\delta i \sim 10^{-10}$ around the transition frequency of the thermal component $x_{\text{th}} \sim 4$. This maximal value corresponds to an annihilating DM of 1 GeV distributed with an NFW profile and observed from our template cluster within an angular resolution of $10''$ (see Eq. 15 and Fig. 1). It is anyway easily rescaled for other configurations.

We also trace in Fig. 6 $\delta i_\chi(x_{\text{th}})/(\tau_\chi m_\chi^n i_0(x_{\text{th}}))$, *i.e.* at the transition frequency of the thermal component, as a function of the DM mass m_χ ; $n=1:2$ for decaying; annihilating DM. We implement the expected mass dependence of the optical depth through the factor of $1/m_\chi^n$. To compare with experimental sensitivities, we have converted our result in terms of the relative intensity shift δi , but only in the case of DM annihilation (look

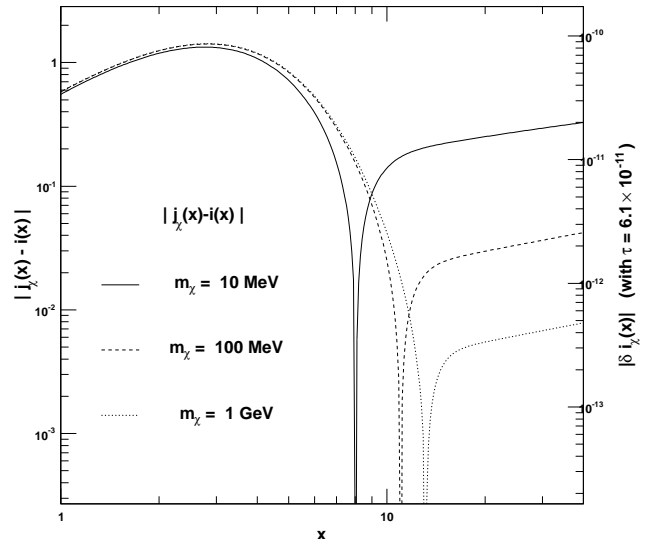


Figure 5: $|\delta i_\chi(x)|/\tau_\chi = |j_\chi(x) - i(x)|$ as a function of the reduced frequency x for different WIMP masses, assuming direct annihilation in e^+e^- (identical for decaying DM, but corresponding to twice the masses). The right vertical axis provides the conversion to $|\delta i_\chi(x)|$ for an optical depth of $\tau = 6.1 \times 10^{-11}$, corresponding to a configuration with 1 GeV annihilating DM with an NFW profile inside our template cluster observed with an angular resolution of $10''$ — see Eq. (15) and Fig. 1.

at the right vertical axis). To do so, we have used the angular average of τ_χ as derived in Eq. (15), which rests on the template DM halo defined in Tab. I. To be consistent with the assumption of annihilation or decay in e^+e^- , however, we have used $N_0 = 2$, and, as discussed above, $\bar{F} = 1$ (*i.e.* for $\tau_{0,\chi}$, we have taken the values of Eq. 16 divided by $5 \cdot 10^3$, which gives $\tau_{0,\chi} = 6.1 \times 10^{-11}$). To switch to the δi associated with DM decay, one may apply a factor of $3.07/2.05 \approx 1.5$ to the right vertical scale (see Eq. 15). Notice that the scaling with m_χ is trivial, $\propto 1/m_\chi^2$ for DM annihilation, and $\propto 1/m_\chi$ for DM decay.

From the results presented in Figs. 5 and 6, it seems quite difficult to detect any SZ signal from DM annihilation or decay, since the typical values obtained for the relative intensity shift is $\delta i_\chi \sim 10^{-10}$, still far from current experimental sensitivities (Planck was optimized for $\delta i \sim 10^{-6}$ [11], *i.e.* the μK level in terms of temperature). However, we remind that this particular value of the intensity shift is connected to some assumptions. For the line-of-sight integral, which depends on the cluster halo properties, we have used $2r_s \mathcal{J} = 10^3$ and 10^5 kpc for DM decay and annihilation, respectively, which corresponds to observing our NFW template cluster within an angular resolution of $\sim 10''$ (see Fig. 1). Moreover, there are additional assumptions on $m_\chi \sim 1$ GeV and on the DM

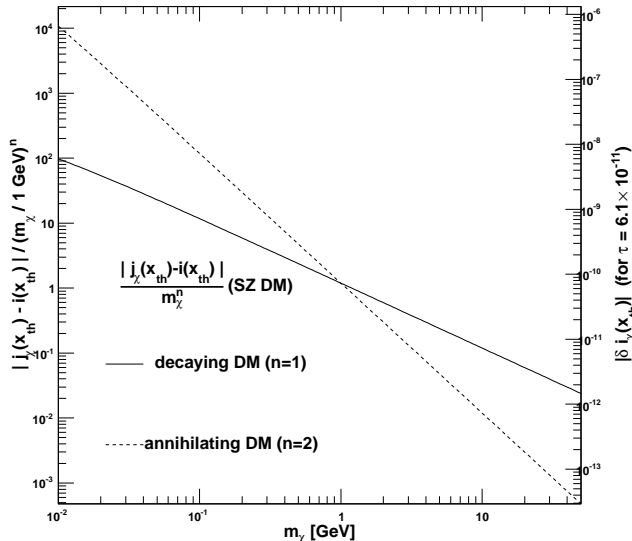


Figure 6: $\delta i_\chi(x_{\text{th}})/(m_\chi^n \tau_\chi)$ as a function of the DM particle mass m_χ , for $x_{\text{th}} = 4$ (left vertical axis). The right vertical axis provides the conversion to $|\delta i_\chi(x_{\text{th}})|$ for an optical depth of $\tau = 6.1 \times 10^{-11}$, corresponding to a configuration with annihilating DM with an NFW profile inside our template cluster observed with an angular resolution of $10''$ — see Eq. (15) and Fig. 1.

properties, while quite generic (see Eq. 15). Anyway, we emphasize that these assumptions are rather optimistic as regards the DM modeling, and should therefore be considered as conservative. For comparison, the intensity shift is shown to be much larger for thermal electrons (see Fig. 3 with the vertical right axis), $\delta i \sim 10^{-4} - 10^{-3}$, over a broad band of frequencies, except at the transition frequency. Hence, the DM effect is likely too small in the major part of the “natural” DM parameter space, but might be still sizable for very light DM candidates and very cuspy profiles.

To figure out the influence of both the DM halo cusps and the experimental angular resolution, one can read off the left vertical axis of Fig. 1, which provides values of the line-of-sight integral for different cluster halo profiles as functions of the angular resolution. To boost our predictions by $\gtrsim 5$ orders of magnitude we would have to consider very cuspy profiles ($\gamma \gtrsim 1.5$) and in the meantime very deep spatial resolutions ($b_{\text{res}} \sim 0.1$ kpc, or equivalently $\theta_{\text{res}} \sim 1''$), at least for the template set of halo parameters of Tab. I.

If we stick to an NFW profile, an alternative to enhance our predictions would be to consider very light annihilating WIMPs, in the sub-GeV mass-scale. However, in the latter case, the value of the annihilation cross considered in Eq. (15) will exceed by a few orders of magnitude the limits coming from not overshooting the DM contribu-

tion to the 511 keV γ -ray line observed in the Galactic center [35, 36], which again points towards other severe limits on the potential SZ signal. Combining very light masses with very cuspy profile seems to be the best possibility for DM to generate an observable SZ distortion of the CMB spectrum, but such an extreme configuration is hardly motivated. Last but not least, one should not forget about the additional foreground coming from other relativistic electrons also injected in clusters from standard astrophysical sources [32]. In any case, any attempt of DM interpretation of any SZ imprints would seem daring. Nevertheless, SZ should still be considered as potentially constraining for unconventional scenarios.

V. CONCLUSION

In this paper, we have revisited the prospect for radio experiments, like Planck or ALMA, for observing SZ distortions of the CMB spectrum due to the presence of relativistic electrons induced by DM annihilation or decay. To this aim, in Sec. III, we have first focused on the most important physical weight on the distortion amplitude, the optical depth associated with the electron density (the thermal background as well as electrons induced by DM annihilation or decay). We have considered typical values for the DM particle properties and a generic template cluster located at a distance of 50 Mpc (Coma lies at ~ 90 Mpc), with features very close to those observed in N-body simulations and a thermal electron population with a density of $n_{e,\text{th}} = 0.01 \text{ cm}^{-3}$, consistent with most of X-ray observations.

We have stressed the importance of the angular resolution inside which the SZ signal has to be averaged, showing that even for very optimistic values of $\sim 1''$, the thermal electron optical depth almost always strongly dominates over that of the DM-induced electrons. This can be interpreted, though very roughly, that the thermal SZ will completely overcome the DM SZ at all frequencies but the thermal transition frequency. In addressing the angular resolution issue, we have derived simple and useful analytical approximations of the line-of-sight integral (Eqs. 20 and 24, the latter being more accurate) that can be used to compute the optical depth for any decaying or annihilating DM model. They are also useful for quick predictions of γ -ray fluxes from DM annihilation or decay in any extragalactic objects, subhalos, dwarf spheroidals, galaxies or clusters.

Finally, we have performed the full spectral analysis of the SZ distortion due to DM-induced electrons in Sec. IV, showing that it can hardly exceed the μK level in terms of temperature fluctuations, except for very extreme cases *e.g.* with very light DM particles, very cuspy cluster halo profiles and large annihilation cross sections or decay rates. Such configurations are not supported by the current studies in each of these specific inputs and, therefore, quite unlikely. Our results are in qualitative agreement with [10], though more accurate and detailed, but

in conflict with the statements made in [5, 6, 7].

Acknowledgments

We are indebted to M. Langer and M. Fairbairn, who initiated the early stages of this work with us. JL is

grateful to LAPTH for hospitality during different stages of this study, and acknowledges financial support by the French ANR project ToolsDMColl (BLAN07-2-194882).

-
- [1] G. Jungman, M. Kamionkowski, and K. Griest, Phys. Rept. **267**, 195 (1996), arXiv:hep-ph/9506380.
- [2] H. Murayama (2007), arXiv:0704.2276.
- [3] C. Boehm and P. Fayet, Nuclear Physics B **683**, 219 (2004), arXiv:hep-ph/0305261.
- [4] P. Salati, PoS **CARGESE2007**, 009 (2007).
- [5] S. Colafrancesco and B. Mele, Astrophys. J. **562**, 24 (2001), arXiv:astro-ph/0008127.
- [6] S. Colafrancesco, Astron. Astrophys. **422**, L23 (2004), arXiv:astro-ph/0405456.
- [7] S. Colafrancesco, S. Profumo, and P. Ullio, Astron. Astrophys. **455**, 21 (2006), arXiv:astro-ph/0507575.
- [8] R. A. Sunyaev and Y. B. Zeldovich, Comments on Astrophysics and Space Physics **4**, 173 (1972).
- [9] R. A. Sunyaev and I. B. Zeldovich, Ann. Rev. Astron. Astrophys. **18**, 537 (1980).
- [10] Q. Yuan, X. Bi, F. Huang, and X. Chen, ArXiv e-prints (2009), arXiv:0902.4294.
- [11] The Planck Collaboration, ArXiv Astrophysics e-prints (2006), arXiv:astro-ph/0604069.
- [12] Science with ALMA, Astrophysics and Space Science **313**, 1 (2008).
- [13] A. Wootten and A. R. Thompson, ArXiv e-prints (2009), arXiv:0904.3739.
- [14] M. Birkinshaw, Phys. Rept. **310**, 97 (1999), arXiv:astro-ph/9808050.
- [15] E. L. Wright, Astrophys. J. **232**, 348 (1979).
- [16] S. Chandrasekhar, *Radiative transfer*. (Oxford, Clarendon Press, 1950., 1950).
- [17] A. Challinor and A. Lasenby, Astrophys. J. **499**, 1 (1998), arXiv:astro-ph/9711161.
- [18] N. Itoh, Y. Kohyama, and S. Nozawa, Astrophys. J. **502**, 7 (1998), arXiv:astro-ph/9712289.
- [19] S. Y. Sazonov and R. A. Sunyaev, Astrophys. J. **508**, 1 (1998).
- [20] A. Stebbins, ArXiv Astrophysics e-prints (1997), arXiv:astro-ph/9709065.
- [21] A. D. Dolgov, S. H. Hansen, S. Pastor, and D. V. Semikoz, Astrophys. J. **554**, 74 (2001), arXiv:astro-ph/0010412.
- [22] C. Boehm and J. Lavalley, Phys. Rev. D **79**, 083505 (2009), arXiv:0812.3282.
- [23] S. Nozawa and Y. Kohyama, Phys. Rev. D **79**, 083005 (2009), arXiv:0902.2595.
- [24] L. Bergström, P. Ullio, and J. H. Buckley, Astroparticle Physics **9**, 137 (1998), arXiv:astro-ph/9712318.
- [25] H. Zhao, MNRAS **278**, 488 (1996), arXiv:astro-ph/9509122.
- [26] J. F. Navarro, C. S. Frenk, and S. D. M. White, Astrophys. J. **490**, 493 (1997), arXiv:astro-ph/9611107.
- [27] B. Moore, F. Governato, T. Quinn, J. Stadel, and G. Lake, Astrophys. J. Lett. **499**, L5 (1998), arXiv:astro-ph/9709051.
- [28] J. S. Bullock, T. S. Kolatt, Y. Sigad, R. S. Somerville, A. V. Kravtsov, A. A. Klypin, J. R. Primack, and A. Dekel, MNRAS **321**, 559 (2001), arXiv:astro-ph/9908159.
- [29] V. S. Berezinsky, A. V. Gurevich, and K. P. Zybin, Physics Letters B **294**, 221 (1992).
- [30] G. Gentile, P. Salucci, U. Klein, D. Vergani, and P. Kalberla, MNRAS **351**, 903 (2004), arXiv:astro-ph/0403154.
- [31] J. F. Navarro, A. Ludlow, V. Springel, J. Wang, M. Vogelsberger, S. D. M. White, A. Jenkins, C. S. Frenk, and A. Helmi, ArXiv e-prints (2008), arXiv:0810.1522.
- [32] T. A. Enßlin and C. R. Kaiser, Astron. Astrophys. **360**, 417 (2000), arXiv:astro-ph/0001429.
- [33] C. L. Sarazin, Astrophys. J. **520**, 529 (1999), arXiv:astro-ph/9901061.
- [34] V. L. Ginzburg, *Theoretical physics and astrophysics* (Oxford: Pergamon, 1979).
- [35] Y. Ascasibar, P. Jean, C. Boehm, and J. Knödseder, MNRAS **368**, 1695 (2006), arXiv:astro-ph/0507142.
- [36] C. Boehm, D. Hooper, J. Silk, M. Casse, and J. Paul, Physical Review Letters **92**, 101301 (2004), arXiv:astro-ph/0309686.